Progress in Organic Coatings 148 (2020) 105827

Contents lists available at ScienceDirect

Progress in Organic Coatings

journal homepage: www.elsevier.com/locate/porgcoat

Study of the anticorrosive properties of "quebracho colorado" extract and its use in a primer for aluminum1050

C. Byrne[a,b], G.J. Selmi[a], O. D'Alessandro[a,b], C. Deyá[a,c,*]

[a] CIDEPINT-CICPBA-CONICET-UNLP Ing., Av. 52 e/ 121 y 122, La Plata, Buenos Aires, Argentina
[b] Departamento de Química, Facultad de Ciencias Exactas, Universidad Nacional de La Plata, 47 y 115 s/nº, La Plata, Buenos Aires, Argentina
[c] Departamento de Ingeniería Química, Facultad de Ingeniería, Universidad Nacional de La Plata, 1 y 47 s/nº, La Plata, Buenos Aires, Argentina

ABSTRACT

Tannins have been used to replace chromate in wash-primers as a temporary ("in transit") protection for metals. In the present work, the anticorrosive properties of "quebracho colorado" tannins were tested in water solution and in wash primers to protect aluminum alloy 1050. Polarization curves (linear and Tafel) and corrosion potential measurements were done on the alloy in contact with different concentrations of the tannin. A tannin wash primer was prepared and coated panels were tested in 100% humidity chamber (ASTM D 2247) and by electrochemical techniques (linear polarization curves, corrosion potentials and ionic resistances). Chromate and talc primers as well as no-coated aluminum alloy were also tested, as control, to compare the results.

1. Introduction

"Quebracho colorado chaqueño" (Schinopsis balansae) and "quebracho colorado santiagueño"(Schinopsis lorentzii) are trees of the Anacardiaceas family native from the Gran Chaco region of Argentina, Paraguay and Bolivia, in South America [1]. "Quebracho colorado" is very appreciated for its hard, heavy, strong wood and its high content of tannins [2,3]. These tannins have been widely used around the world for the industrial production of leather [4]."Quebracho colorado" tannins are a complex combination of polyphenols obtained by extraction from the trees heartwood [5]. These are condensed tannins (proanthocyanidins) of the profisetinidine type [6–10], which are constituted by units of the flavan-3,4-diol leucofisetinidin [1,11]. The natural, common or ordinary extract is obtained by direct extraction of quebracho wood with boiling water. This extraction causes the hydrolysis of heterocyclic rings, which results in the formation of condensation products called phlobaphenes or red tannins, which are soluble in hot water, but hardly soluble in cold water [7,12]. To obtain cold-soluble quebracho extracts, it is necessary to submit the ordinary extract to a sulphitation process that transforms the phlobaphenes into completely soluble tannins [1,13]. The cold-water-soluble quebracho extracts are the most known and used types of quebracho extracts.

During the last decades, research on the alternative uses of tannins allowed its incorporation in a growing number of applications. Tannins can retard the corrosion reactions of metals by adsorbing on their surfaces through the electron rich oxygen atoms in their structures [14], so the application of tannins in corrosion studies has been widely investigated [15]. Most corrosion researches of tannins involve their anticorrosive properties on steel [16] or as rust converters [17–19]. Some researchers worked on tannin solution [20–24] or with natural extracts containing tannins [25] or in anticorrosive primers [17,21,26–30] and paints [28,31] to protect steel.

Similarly, many researchers have studied tannins from different sources as green inhibitors for aluminum alloys. Mimosa tannins were studied as an inhibitor on the corrosion of AA6060 aluminum alloy in acid rain solution [32] while *Acacia mearnsii* tannin was studied on AA7075-T6 in 0.1 M HCl solution [33] and on AA1200 in 3.5% NaCl solution [34]. Yahya investigated the ability of *Rhizophora apiculata* tannins to minimize the corrosion rate of Al alloys in NaCl solutions [35]. Likewise, Nnaji studied the red onion (*Allium cepa*) skin tannin and the cashew nut (*Anacardium occidentale*) testa tannin as corrosion inhibitors of aluminum in hydrochloric acid solutions [36,37]. However, there are no reports in the literature about the anticorrosive action of quebracho tannins on aluminum alloys.

In the present work, the anticorrosive properties of different suspensions of "quebracho colorado" tannins extract on 1050 aluminum alloy were first analyzed, and then the extract was used in the formulation of an anticorrosive primer (temporary protection [38]). This work constitutes, therefore, the first study reported on the use of "quebracho colorado" tannins as corrosion inhibitors of aluminum and its application in temporary protective coatings on this metal.

* Corresponding author at: CIDEPINT-CICPBA-CONICET-UNLP Ing., Av. 52 e/ 121 y 122, La Plata, Buenos Aires, Argentina.
E-mail address: c.deya@cidepint.ing.unlp.edu.ar (C. Deyá).

https://doi.org/10.1016/j.porgcoat.2020.105827
Received 11 November 2019; Received in revised form 1 June 2020; Accepted 6 June 2020

2. Experimental

2.1. Characterization of the "quebracho colorado" extract

2.1.1. Generalities

The commercial cold-water-soluble extract UNITAN ATO was used as quebracho tannin source. This product is a dry spray of "quebracho colorado" wood extract (*Schinopsis balansae / lorentzii*), treated with sodium bisulphite. It is a fine and homogeneous reddish brown powder, which according to the manufacturer [39] has 72 ± 2% tannins, determined by the official method of the Society of Leather Technologists and Chemists [40], 20 ± 1% non-tannin compounds, 8 ± 0.5% humidity and 0.2% insoluble compounds.

The pH of a 0.5% w/v quebracho extract suspension was determined with a portable pH meter CONSORT P500.

2.1.2. Total soluble polyphenols

The Folin–Denis method was used for analyzing total soluble polyphenols present in the quebracho extract [26,41,42]. The quebracho extract was dissolved in water at 20 °C (0.5 g in 100 mL), left to equilibrate for 24 at 300 rpm and then filtered by filter paper Schleicher & Schuell 589 medium pore. The supernatant was diluted 1/100 and used to determine soluble polyphenols. Folin–Denis reagent was prepared by dissolving 10.0 g of sodium tungstate ($Na_2WO_4{\cdot}2H_2O$), 2.0 g of phosphomolybdic acid ($H_3P(Mo_3O_{10})_4{\cdot}H_2O$) and 5.0 mL H_3PO_4 in 80 mL of deionized water, at boiling temperature. After cooling, the final volume was adjusted to 100 mL. Tannic acid was used as the standard for polyphenols. Standard solutions of tannic acid, containing 1.0, 2.0, 4.0, 5.0, 6.0, 7.0 and 10.0 ppm, were prepared from a stock solution. The tannic acid solution was mixed with 2.0 mL of saturated Na_2CO_3 solution and 2.0 mL of the Folin–Denis reagent; then, the final volume was adjusted to 25.0 mL with distilled water. The reaction was completed after 15 min, and absorbance measurements were performed at 750 nm using a Spectrum SP 2000 UV spectrophotometer. The total phenols were estimated as tannic acid equivalent.

2.1.3. FTIR spectrum

The commercial extract was characterized by Fourier Transform Infrared Spectroscopy (FTIR). The extract was thoroughly mixed with KBr, pressed into a pellet and the FTIR spectrum was then recorded by a Perkin Elmer Spectrum One Spectrometer within the range of 450 and 4000 cm^{-1} wave number. A resolution of 4 cm^{-1} with 12 scans was used.

2.2. Study of the anticorrosive properties of the "quebracho colorado" extract

The electrochemical evaluation of the quebracho extract inhibitory capacity was carried out through the study of polarization curves, corrosion potential measurements (Ec) and corrosion current density (Ic) determination by means of linear polarization tests.

2.2.1. Preparation of the substrate

Commercially pure aluminum 1050 cylindrical electrodes were used as working electrodes. Just before immersion, the electrodes were sanded successively with 220, 320, 360 and 600 grain size wet emery paper. The electrodes were immersed in different quebracho extract suspensions (0.005, 0.01, 0.05, 0.1, 0.3 and 0.5% w/v) in 0.1 M NaCl, stirred at 300 rpm. For polarization studies, a set of three Al electrodes were used for each exposure time, and mean values are presented.

2.2.2. Linear polarization curves

Linear polarization tests [43] were carried out at 2, 5 and 24 h with a Gamry Interface 1000 potentiostat, selecting a scanning range of ± 20 mV from the open circuit potential and using a scanning rate of 0.25 $mV{\cdot}s^{-1}$. The cell used consisted of a 1050 aluminum electrode of 0.28 cm^2 exposed area, a Pt electrode as a counter electrode and saturated calomel electrode (SCE) as reference. Ic was determined by the software Gamry Echem Analyst Version 6.33. The inhibition efficiency IE was calculated according to the following equation [33,36]:

$$IE = \frac{I_0 - I}{I_0} \cdot 100 \quad (1)$$

where I_0 indicates the Ic of the blank, that is, aluminum immersed in 0.1 M NaCl solution without extract addition, while I is the Ic of the metal in the corresponding quebracho extract suspensions.

2.2.3. Potentiodynamic polarization curves

The potentiodynamic polarization curves at 2 and 24 h were obtained using a cell identical to the one described above, using a potential range of ± 250 mV from the open circuit potential and a scanning rate of 1 $mV{\cdot}s^{-1}$. Anodic and cathodic Tafel slopes were determined from these E-log I curves.

2.2.4. Corrosion potential measurements

The corrosion potential was measured every 10 min for 4 h using an aluminum 1050 electrode of 1.33 cm^2 area and an SCE as reference. Once the Ec determination tests were completed, the immersed extreme of the electrode was cut to study the exposed surface by scanning electron microscopy (SEM), and its composition was determined by means energy dispersive X-ray microanalysis (EDS). The equipment used was a Philips SEM 505 microscope and an EDAX DX PRIME 10 energy dispersive micro-analyzer.

2.3. Formulation, preparation and application of an anticorrosive primer based on quebracho extract

A primer based on quebracho extract (TQ primer) was developed and its anticorrosive efficiency was compared with a primer that possesses zinc tetroxychromate (SNCZ provided by) as anticorrosive pigment (CR primer) and with another in which the anticorrosive pigment is replaced by talc (TAL primer).

The primers (Table 1) were formulated by a two-pack system, A and B, which are stored separately and mixed (4 parts of A and 1 part of B, by weight), immediately before application. Part A includes the anticorrosive pigment (quebracho extract or zinc tetroxychromate), the filler (talc), the prime pigment (carbon black), the resin (film-forming material, in this case Butvar® B-76, a thermoplastic polyvinyl butyral resin), the organic solvents to adjust the viscosity (isopropanol and 1-butanol) and water, while part B contains isopropanol, water and

Table 1
Formulation of the different tested primers.

PART A			
Component	% volume		
	TQ	CR	TAL
Polyvinylbutyral resin	8.18	8.18	8.18
Pigment	2.21	2.21	–
Talc	0.47	0.47	2.68
Carbon black	0.05	0.05	0.05
1-butanol	22.89	22.89	22.89
Isopropanol	64.06	64.06	64.06
Water	2.14	2.14	2.14
PVC	0.22	0.22	0.22

PART B	
Component	% volume
Phosphoric acid (85%)	9.0
Water	15.2
Isopropanol	75.8

PVC Pigment volume concentration.

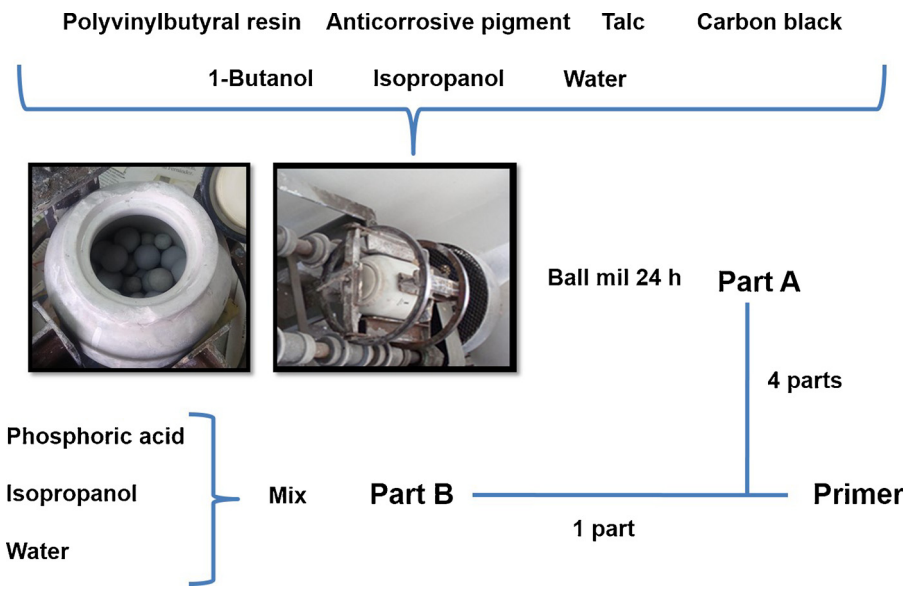

Fig. 1. Flow chart of paint preparation.

phosphoric acid, being the last one essential to provide good adhesion to the substrate (Fig. 1).

A set of AA 1050 panels (75 × 75 x 1 mm) was degreased with isopropanol and coated with the primers, by brush, up to a dry film thickness of 8 ± 2 µm. The film thickness was measured with a Schwyz SC117-02 Coating Thickness Gauge. Then they are cured for 5 days at 20 ± 2 °C and 70% RH.

2.4. Evaluation of the coated panels

2.4.1. Humidity chamber

A set of three of each type of coated panels was placed in the humidity chamber (ASTM D 2247) [44] in order to evaluate the adhesion (ASTM D 3359) [45], the blistering degree (ASTM D 714) [46] and the eventual presence of corrosion along time. For this last, we use the visual corrosion classification scale of aluminum that is specified in Table 2 [47]. After humidity chamber exposure, the film of the coated panels was removed mechanically with a lab spatula and the surface was analyzed by scanning electron microscopy coupled to energy-dispersive X-ray spectroscopy (SEM-EDS).

2.4.2. Electrochemical tests

Electrochemical assessment of coated panels was carried out by means of D.C. electrochemical techniques. The employment of these techniques was justified by the low ionic resistance of the primer film [48,49].

Electrochemical tests were done on cells obtained by fixing a cylinder, 2 cm diameter, on the painted specimen and filled with 0.1 M sodium chloride as electrolyte. The ionic resistance (Ri) was calculated from conductivity (Ci) as

$$Ri = Ci^{-1} \quad (2)$$

Table 2
Visual classification scale of aluminum corrosion.

Classification	Description
No appreciable attack (N)	There is no appreciable attack; the surface may be discolored
Pitting (P)	Discrete pits
Filiform (F)	Presence of corrosion filaments
General (G)	Fairly uniform corrosion with accumulation of powdery corrosion products
Exfoliation (E)	Visible metal separation in layers

Ci measurements were done using a Pt counter electrode and an ATI ORION model 170 conductimeter which operates at 1000 Hz. The polarization resistance without IR compensation (Rp) was determined by the linear polarization technique (± 20 mV from open circuit potential, scan rate 1 $mV{\cdot}s^{-1}$) with a Gamry Interface 1000 potentiostate, employing a typical three electrodes cell, with a Pt counter electrode and a SCE as reference. For corrosion potential (Ec) measurements the SCE was used as reference.

Tests were done by triplicate.

3. Results and discussion

3.1. Characterization of the "quebracho colorado" extract

3.1.1. Generalities

The pH of a 0.5% w/v suspension of the extract was 4.4, value that is within the range provided by the manufacturer [39].

3.1.2. Total soluble polyphenols

The absorbance of the extract solution, using the Folin-Denis method, was 0.22; then, considering the calibration curve obtained for the absorbance determination with Folin-Denis reactant and the dilution prepared, the content of total soluble polyphenols was 3.74 ppm, corresponding to 75 mg of tannic acid per gram of extract.

3.1.3. FTIR spectrum

The FTIR spectrum of the "quebracho colorado" extract is showed on Fig. 2, and the assignment of each band is resumed on Table 3 [6,50–54]. The 1283 cm^{-1} strong band is a characteristic feature for the flavonoid-based tannins, and can be assigned to the ethereal C—O asymmetric stretching vibration arising from the pyran-derived ring structure of this class of tannins. The typical strong band at 1731-1704 cm^{-1} of hydrolysable tannins [6,51], assigned to the stretching vibration of the carbonyl function, is not present, confirming that the tannin belongs to the non-condensable family.

3.2. Study of the anticorrosive properties of the "quebracho colorado" extract

The inhibition efficiency along time of the "quebracho colorado" extract suspensions is shown on Fig. 3. The inhibition efficiency, calculated from corrosion currents (Ic, Table 4), increases with the

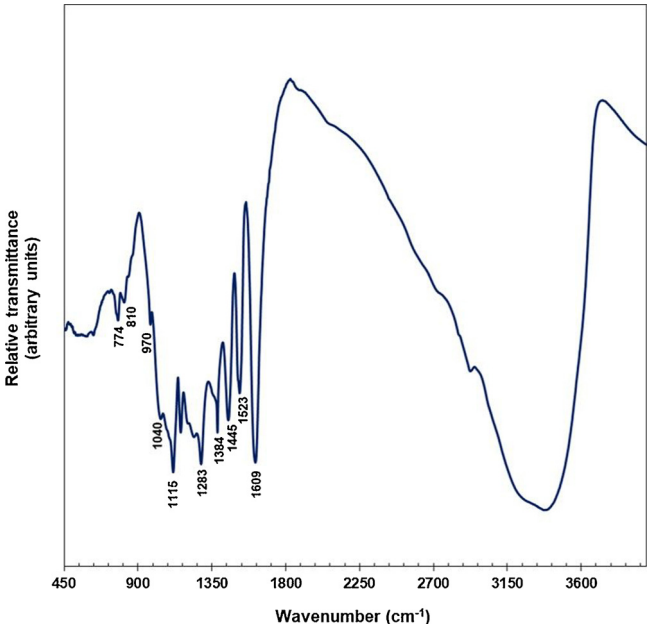

Fig. 2. FTIR spectrum of the "quebracho colorado" extract.

Table 3
Assignments of the FTIR bands in the "quebracho colorado" extract.

Band (cm^{-1})	Assignment
774	C–H deformation out of plane
810	
970	C–O stretching of the multiple hydroxyl groups
1040	
1115	C–H deformation in plane
1283	C–O stretching of the heterocyclic ring of the flavonoids that
1384	constitute the polymer structure of condensed tannins
1445	stretching of C = C– aromatic groups
1523	
1609	
3000-3600	Sum of different vibrational bands of –OH groups

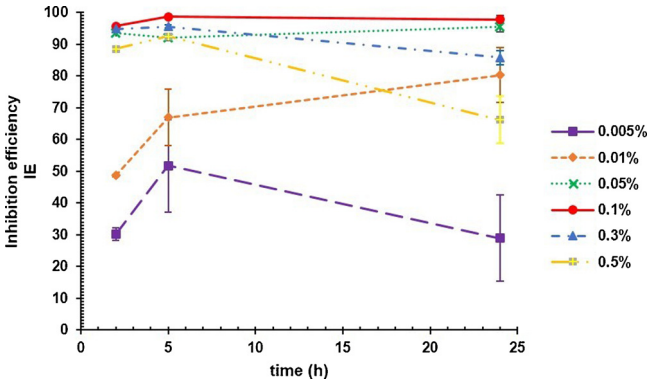

Fig. 3. Inhibition efficiency (IE) as function of time for the "quebracho colorado" extract suspensions.

concentration of the extract until reaching a maximum (95–99%) with the 0.1% suspension, then decreasing as the concentration increases.

Potentiodynamic polarization curves for AA 1050 immersed 2 h in the "quebracho colorado" extract suspensions in NaCl 0.1 M can be seen in Fig. 4. A decrease in both anodic and cathodic branch is observed. This mixed inhibition is consistent with the mechanism of film formation that is characteristic of many organic inhibitors, where a hydrophobic protective film is formed on the surface that blocks both anodic and cathodic areas [35,55]. In aerated solutions the cathodic reaction is

Table 4
Kinetics parameters of corrosion obtained by linear polarization and Tafel extrapolation tests on aluminum 1050 exposed 2 h to different quebracho extract suspensions in NaCl 0.1 M.

Quebracho extract concentration (% w/v)	Linear polarization tests	Potentiodynamic polarization curves (Tafel)		
	I_c (A/cm^2)	$-b_d$ (mV)	b_a(mV)	I_c (A/cm^2)
0	$5.7{\cdot}10^{-5}$	625	71	$5.7{\cdot}10^{-5}$
0.005	$3.9{\cdot}10^{-5}$	625	56	$1.9{\cdot}10^{-5}$
0.01	$2.9{\cdot}10^{-5}$	625	53	$1.1{\cdot}10^{-5}$
0.05	$3.6{\cdot}10^{-6}$	500	45	$4.1{\cdot}10^{-6}$
0.1	$2.5{\cdot}10^{-6}$	667	48	$8.9{\cdot}10^{-6}$
0.3	$3.8\ 10^{-6}$	588	56	$1.7{\cdot}10^{-5}$
0.5	$6.5{\cdot}10^{-6}$	769	59	$2.4{\cdot}10^{-5}$

dominated by the diffusion and the reduction of dissolved oxygen [56], so the organic film slows down this process. In Fig. 4 it is observed that the cathodic current density decreases as the extract concentration increases, until reaching a minimum for the 0.05% concentration; then the current density increases with the increase in concentration. In NaCl solutions the anodic reaction is the dissolution of aluminum catalyzed by Cl^- ions as no passive film can be formed in this aggressive media [43,57]. In the presence of tannins, the film formed on Al would interfere with both the adsorption of Cl- ions and the diffusion of Al^{3+} ions from the metal surface to the bulk solution [58]. It can be seen in Fig. 4 that the anodic current density has a similar tendency than the cathodic branch, reaching a minimum for the 0.05% concentration. Besides, the cathodic reaction (reduction of O_2) has a diffusion control, while the aluminum dissolution is activation-controlled [43]. In Fig.4 is also clear that although the corrosion current varies with tannin concentration, Tafel slops are similar. Moreover, no passive region was observed indicating that the protection is due to the accumulation of tannin at the alloy / solution interface or its adsorption on the surface [35].

As the cathodic reaction is O_2 reduction, OH^- are formed during cathodic polarization and pH changes occurred on the electrode surface during cathodic polarization [59].

The cathodic Tafel slopes cannot be determined as the kinetics of the reaction is control by diffusion; however, the slopes of the curves (b_d) were obtained between -50 to −250 mV and the corrosion current density (Ic) was determined as the diffusion current density [59].

In the curves, it can also be seen that at low anodic overpotential the Tafel relationship is followed, showing that anodic reaction is activation-controlled, but at higher anodic overvoltage a limiting diffusion current appears on the anodic polarization curves showing that at higher current densities, the transport of ions towards the electrode surface becomes the rate-determining step (concentration polarization) [43]. The corresponding Tafel parameters (Table 4) were obtained employing polarization data near the corrosion potential (between 50–100 mV in the anodic curves).

Polarization curves after 24 h of immersion (Fig. I, Supplementary data) show an almost complete loss of cathodic inhibition and a not so marked decrease in anodic current density, especially for higher tannin concentration. This may be due to two effects, the films became more permeable to oxygen and chloride ions and the reaction of O_2 alkalinized the cathodic sites producing a less effective interaction between Al and tannin [24,35,36].

A difference was observed between the open circuit potential (OCP) and the corrosion potential (Ec) obtained by Tafel curves (ΔE ~ 30 mV). These differences may be due to the disturbance of the charging current [60,61]. Besides this difference results in an asymmetric overvoltage as ± 250 mV was applied from OCP and η was calculated as

$$\eta = E - Ec \quad (3)$$

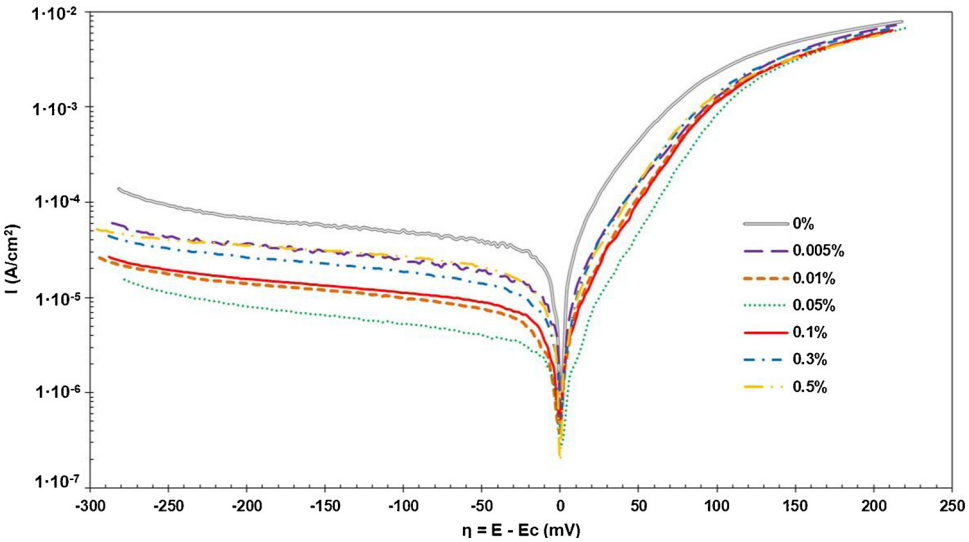

Fig. 4. Potentiodynamic polarization curves for Al 1050 immersed 2 h in the "quebracho colorado" extract suspensions.

being η the overpotential, E the applied potential and Ec the corrosion potential.

Fig. 5 shows the variation of the corrosion potential as a function of time for the different extract concentrations. During the first 30 min, AA1050 immersed in the tannin suspensions had more negative potential values than those of the blank test, without a clear dependence on the concentration. These negative values, which indicate an active metallic surface, moves towards more positive ones as the film formation takes place [62]. After 90 min and until the end of the test the suspensions provide slightly more positive potential values than those of the blank, being more positive as the concentration of the extract increased. These constant potential values indicate that the film formed is been stabilized [62].

The evaluation by SEM of the aluminum surface exposed to 0.1% of tannin suspension for 4 h shows the formation of a film with numerous cracks and fissures (Fig. 6).The analysis by EDS of this film shows the presence of both C and O, which confirms the organic nature of the film. The maximum inhibitory efficiency of the 0.1% suspension would be explained by the formation of a film with the best protective characteristics.

According to these results, it can be seen that the best inhibition is achieved when the concentration of tannin is 0.05-0.1%. At lower concentration, the film formed does not block the reaction sites properly. At higher concentration there are probable packing interferences among the tannins molecules due to steric impediments and the film formed is not as compact as at lower concentrations [36] or / and soluble oligomers are formed [24]. Similar results were obtained using cashew nut testa tannin on aluminum [36] and quebracho tannin (Schinopsis sp.) [21] and Mangrove tannins on steel [24].

The polarization kinetics parameters agree with those of Tafel curves except at higher concentrations maybe due to changes in the organic film on aluminum caused by the overpotentials applied during Tafel polarization curves.

3.3. Evaluation of the coated panels

3.3.1. Humidity chamber

TQ primer presented an adhesion similar to that of the CR control: quite good at the beginning (4B), regular (3B) after 1 day in the chamber and poor (2B) after 5 days (Table 5). The talc primer also presented good adhesion (4B) at the beginning, but the adhesion was completely lost after just one day in the chamber.

TQ and CR panels showed no appreciable attack after 21 days in the chamber, while the TAL panels presented pitting after 8 days and general corrosion after 21 days in the chamber (Table 5, Fig. II-V Supplementary data).

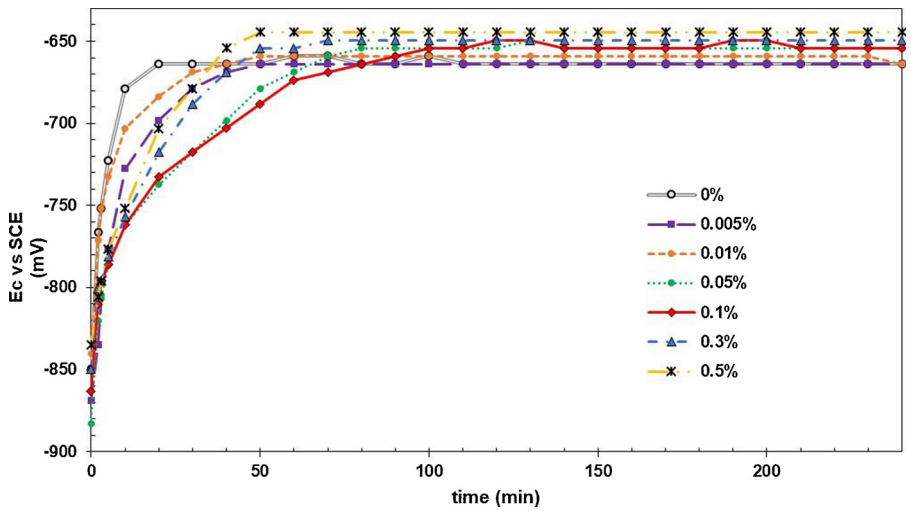

Fig. 5. Corrosion potential (Ec) as function of time for Al 1050 immersed in the "quebracho colorado" extract suspensions.

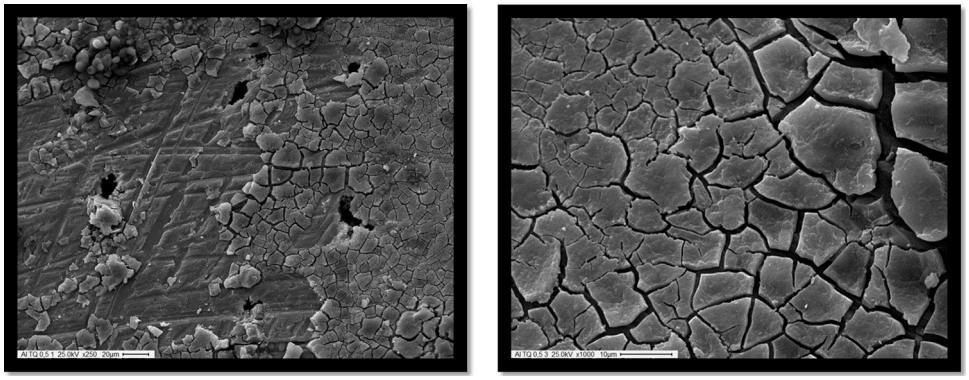

Fig. 6. SEM micrographs of the aluminum surface exposed to a suspension 0.1% quebracho extract for 4 h: 500X (left) and 1000X (right).

Table 5
Humidity chamber. Adhesion degree and visual classification of aluminum corrosion.

Primer	Adhesion grade (ASTM D 3359)*			Visual classification of corrosion**			
	Time (days)			Time (days)			
	0	1	5	4	8	14	21
TQ	4B	3B	2B	N	N	N	N
CR	4B	3B	2B	N	N	N	N
TAL	4B	0B	0B	N	P	P	G
B	–	–	–	G	G	G	G

* 4B: less than 5%; 3B: between 5 and 15%; 2B: between 15 and 35%; 0B greater than 65% of the painted area was removed.

** N: No appreciable attack; P: Pitting; F: Filiform; G: General; E: Exfoliation.

Table 6
EDS analysis on aluminum samples.

			Elements (weight %)						
			Al	O	Fe	C	P	Ca	K
Samples exposed in the humidity chamber and unpainted	TQ	Zone I	91.61	5.29	0.45	2.65			
		Zone II	65.70	25.47	0.37	2.94	4.97	0.21	0.34
	CR		93.82	1.94	0.52	3.72			
	TAL	Zone I	88.73	7.41	0.38	2.69	0.78		
		Zone II	66.75	24.60	0.43	3.38	4.20	0.55	0.09
	B		59.56	40.44					
Unexposed Al 1050			97.8	1.88	0.32				

All the samples presented no blisters along the assay.

The EDS analysis of the surfaces after humidity chamber exposure is shown on Table 6. The TQ coated panels presented two zones (Fig. 7): zone I with an homogenously layer and the other (zone II) with a cracked layer on top of the homogenously one. In zone I, the layer contains Al and O as main compounds. In zone II, the upper layer contains C and P indicating a good adhesion of the primer to the aluminum surface. In the case of CR, the primer could not be completely removed. Its surface showed a uniform aspect, with the presence of C that denotes good adhesion, but no evidence of P (Fig. 8). The TAL panels showed a similar layout (Fig. 9), with an area of homogenous layer and other area with two layers. In this case, the upper layer is less compact than in the case of TQ panels. The surface of the uncoated aluminum (B) showed formations with Al and O quantities (Table 6) and structures that indicate the formation of a thick layer of alumina (Fig. 10) [53,63].

3.3.2. Electrochemical studies

3.3.2.1. Ionic resistance determinations. The TQ coated panels presented Ri values between 5000 and 10,000 Ω·cm^2 throughout the experiment (Fig. 11). The TAL panels presented values similar to TQ during the first 100 h, and then the values increased until reaching a maximum of 15,000 Ω·cm^2 after 350 h of immersion. At the beginning of the exposure the CR coated panels presented ionic resistance higher than those corresponding to the other panels, reaching a maximum of 33,000 Ω·cm^2 after 100 h, but then decreased to 10,000 Ω·cm^2 after 350 h, keeping this value up to the end of the test.

It can be seen that the ionic resistance for all the coated panels was low (between 10^3 and 10^4 Ω·cm^2). This indicates a poor barrier effect, which is characteristic of these temporary protectors.

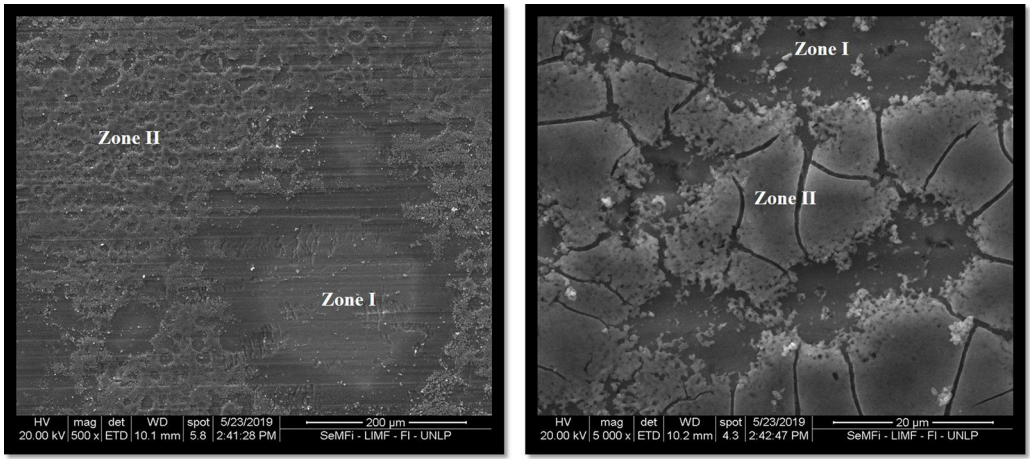

Fig. 7. SEM micrographs of the TQ coated panels after humidity chamber exposure: 500X (left) and 5000X (right).

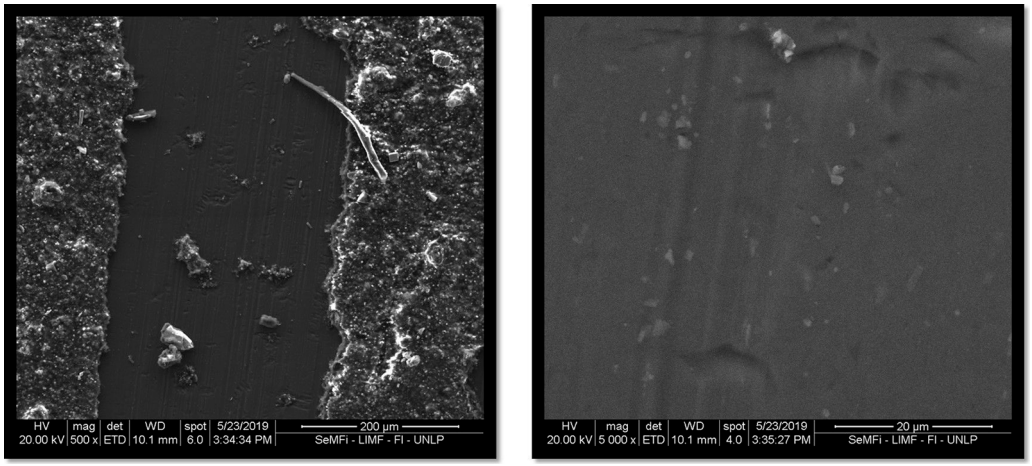

Fig. 8. SEM micrographs of the CR coated panels after humidity chamber exposure: 500X (left) and 5000X (right).

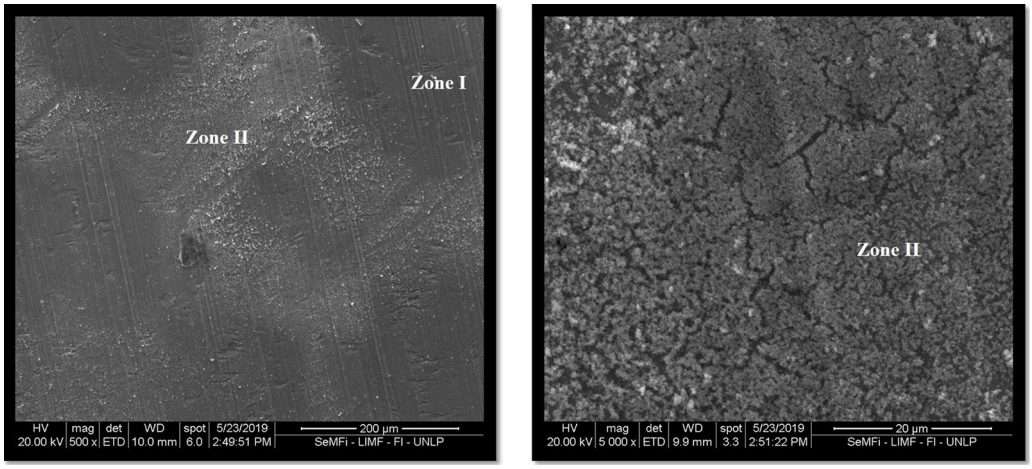

Fig. 9. SEM micrographs of the TAL coated panels after humidity chamber exposure: 500X (left) and 5000X (right).

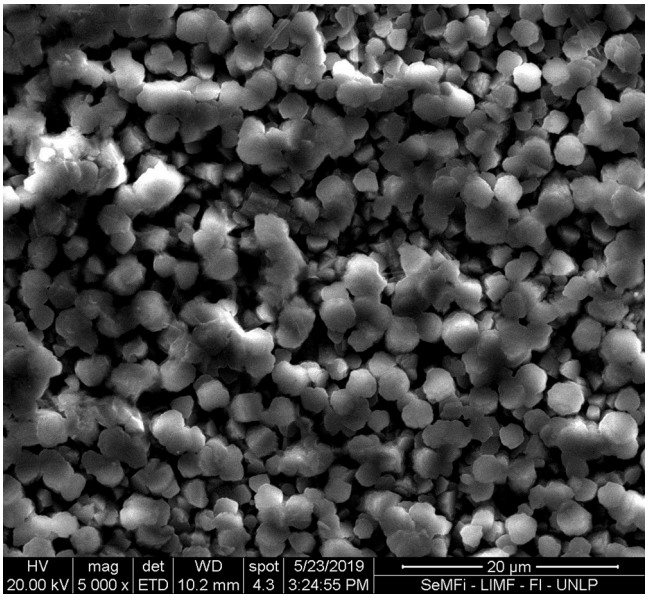

Fig. 10. SEM micrographs of the B panels after humidity chamber exposure: 500X (left), and 5000X (right).

3.3.2.2. Polarization resistance determinations. The TQ coated panels presented Rp values that increased from $5.5{\cdot}10^5 \Omega{\cdot}cm^2$ at the beginning to $\sim 10^7 \Omega{\cdot}cm^2$ at 200 h, keeping along this value until 700 h (Fig. 12). Both the TAL coated panels and the uncoated aluminum showed a similar behavior: Rp increased from the beginning up to 100 h exposure, reaching values that were maintained in the order of $10^6 \Omega{\cdot}cm^2$ for the rest of the experiment. CR coated panels presented Rp values in the order of $10^7 \Omega{\cdot}cm^2$ throughout the test.

It can therefore be seen that although CR panel always has the highest Rp values, TQ panels has Rp values very similar to CR after 200 h of exposure. In the supplementary data Fig. VI shows some of these curves.

3.3.2.3. Corrosion potential measurements. The uncoated aluminum presented the most negative Ec, with values lower than −800 mV during the first 4 h and in the range of -700 to −800 mV during the rest of the test (Fig. 13). The TQ panels showed Ec values in the range of -600 to −700 mV during the first 200 h, and in the range of -500 to −600 mV up to the end of the experiment. During the first 24 h the TAL panels presented values slightly more positive than TQ, but then they became more negative, with values in the range of -700 to −800 mV. The CR panels presented the most positive values during the first hours of testing, but after 200 h the values were in the same interval as those corresponding to TQ.

According to the results of the tests on the coated panels, the replacement of chromate pigment by tannin in the primer results in good protection in the humidity chamber as the adhesion and the corrosion

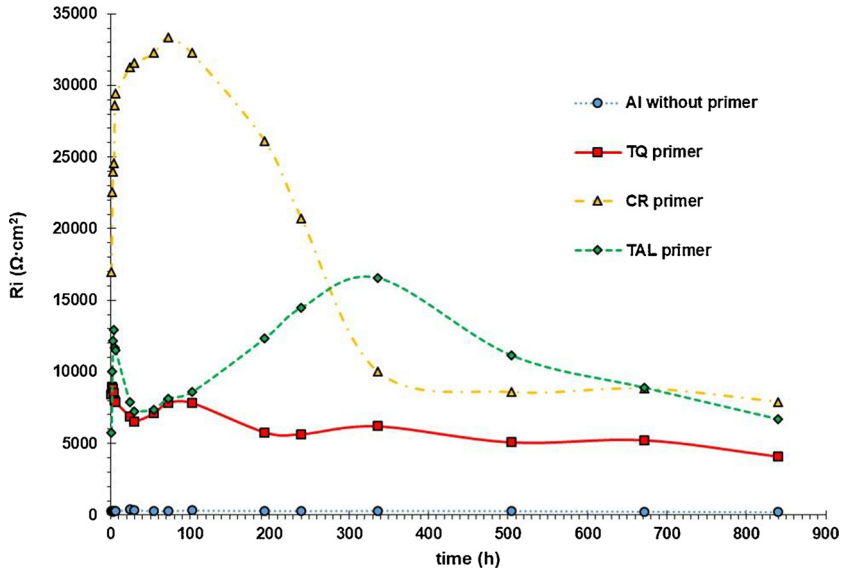

Fig. 11. Ionic resistance values (Ri) as function of time for coated panels.

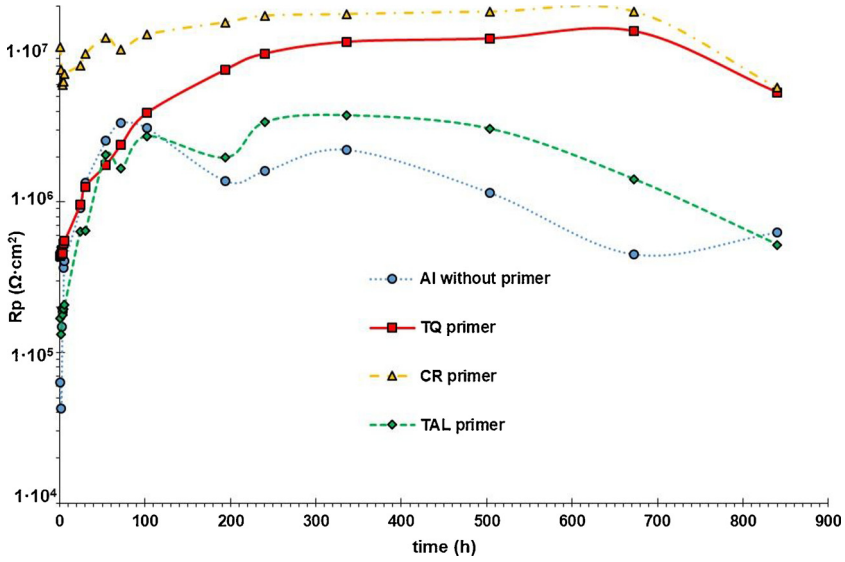

Fig. 12. Polarization resistance values (Rp) as function of time for coated panels.

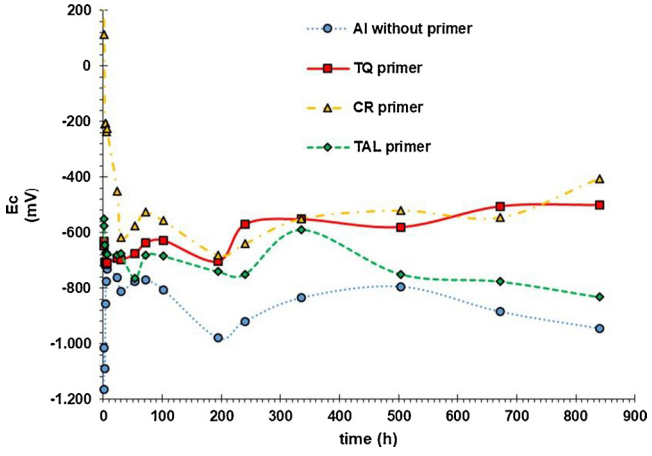

Fig. 13. Corrosion potential values (Ec) as function of time for coated panels.

degree were similar for both primers. The replacement of chromate by talc results in poor protective behavior, probable due to the formation of a less compact layer on the aluminum. In the case of TQ, the ionic resistance is slightly lower than chromate primer, indicating that the barrier properties are also lower. However, polarization resistance and corrosion potential evolution against time were similar indicating that once water penetrates the coating, tannin pigment is able to protect aluminum as chromate does.

4. Conclusions

Quebracho tannin in solution protects aluminum depending on the tannin concentration, being the best protection afforded by concentration 0.05 - 0.1%. This protection is partially lost after 24 h. The formation of an organic inhibitor film on the Al surface by the quebracho tannin reduces the active surface area available for the attack of the corrosive medium and delays oxygen reduction and metal dissolution.

Quebracho tannin can be used to prepare primers for aluminum substrate and can replace chromate as anticorrosive pigment as they

afford similar protection. Despite the barrier properties of tannin primer are lower than that of chromate one, once water penetrates the coating, tannin protects aluminum in a similar degree than chromate.

Availably data

All data included in this study are available upon request by contact with the corresponding author.

CRediT authorship contribution statement

C. Byrne: Investigation, Writing - original draft. **G.J. Selmi:** Validation. **O. D'Alessandro:** Conceptualization, Methodology, Resources, Data curation, Visualization, Project administration. **C. Deyá:** Writing - review & editing, Supervision, Funding acquisition.

Declaration of Competing Interest

The authors declare that they have no known competing financial interests or personal relationships that could have appeared to influence the work reported in this paper.

Acknowledgements

The authors are grateful to CONICET (Consejo Nacional de Investigaciones Científicas y Técnicas), UNLP (Universidad Nacional de La Plata) and CICPBA (Comisión de Investigaciones Científicas de la Provincia de Buenos Aires) for their sponsorship to do this research.

Appendix A. Supplementary data

Supplementary material related to this article can be found, in the online version, at doi:https://doi.org/10.1016/j.porgcoat.2020.105827.

References

[1] P.B. Venter, M. Sisa, M.J. van der Merwe, S.L. Bonnet, J.H. van der Westhuizen, Analysis of commercial proanthocyanidins. Part 1: the chemical composition of quebracho (Schinopsis lorentzii and Schinopsis balansae) heartwood extract, Phytochemistry 73 (2012) 95–105.
[2] C. Alzugaray, N.J. Carnevale, A.R. Salinas, Growth in samplings of Schinopsis balansae engl, ECOTROPICA 14 (2008) 27–35.
[3] W. Streit, D. Fengel, Formation and deposition of tannins in Quebracho colorado (Schinopsis balansae Engl.), Holz Als Roh- Und Werkst. 53 (1995) 56–60.
[4] G. Griyanitasari, I.F. Pahlawan, E. Kasmudjiastuti, Thermal stability of shoe upper leather: comparison of chestnut and quebracho as vegetable tanning agent, IOP Conference Series: Materials Science and Engineering 432 (2018) 012040.
[5] H.R. Di Rado, V.E. Fabre, F.D. Miño, Estabilización de suelos con taninos, Inf. Tecnolã³gica 12 (2001) 7–14.
[6] L. Falcão, M. Araújo, Vegetable tannins used in the manufacture of historic leathers, Molecules 23 (2018) 1081.
[7] A. Pizzi, K.L. Mittal, Natural phenolic adhesives derived from tannins and lignin, in: A. Pizzi, K.L. Mittal (Eds.), Handbook of Adhesive Technology, CRC Press, 2017, pp. 263–282.
[8] S. Quideau, D. Deffieux, C. Douat-Casassus, L. Pouysegu, Plant polyphenols: chemical properties, biological activities, and synthesis, Angew. Chemie 50 (2011) 586–621.
[9] Y. Shirmohammadli, D. Efhamisisi, A. Pizzi, Tannins as a sustainable raw material for green chemistry: a review, Ind. Crops Prod. 126 (2018) 316–332.
[10] W. Streit, D. Fengel, Purified tannins from quebradho colorado, Phytochemistry 24 (1994) 481–484.
[11] D.G. Roux, S.R. Evelyn, Condensed tannins. 2. Biogenesis of condensed tannins based on leucoanthocyanins, Biochem. J. 70 (1958) 344–349.
[12] H.G. Bennett, The manufacture of leather, constable & company ltd, London (1920).
[13] M. Kardel, F. Taube, H. Schulz, W. Schütze, M. Gierus, Different approaches to evaluate tannin content and structure of selected plant extracts – review and new aspects, J. Appl. Bot. Food Qual. 86 (2013) 154–166.
[14] M. Oki, Performance of Tannin/Glycerol-Chromate hybrid conversion coating on aluminium, J. Mater. Sci. Chem. Eng. 03 (2015) 1–6.
[15] A. Pizzi, Tannins: Prospectives and Actual Industrial Applications, Biomolecules 9 (2019) 344–373.
[16] A.A. Rahim, J. Kassim, Recent development of vegetal tannins in corrosion protection of Iron and steel, Recent. Pat. Mater. Sci. 100 (2008) 223–231.
[17] C. Byrne, O. D'Alessandro, G.J. Selmi, R. Romagnoli, C. Deyá, Primers based on tara and quebracho tannins for poorly prepared steel surfaces, Prog. Org. Coat. 130 (2019) 244–250.
[18] A.A. Rahim, M.J. Kassim, E. Rocca, J. Steinmetz, Mangrove (Rhizophora apiculata) tannins: an eco-friendly rust converter, Corros. Eng. Sci. Technol. 46 (2011) 425–431.
[19] V.S. Saji, Progress in rust converters, Prog. Org. Coat. 127 (2019) 88–99.
[20] A. Abdulmajid, T. Sherwyn Hamido, A.A. Rahim, M.H. Hussin, Tamarind shell tannin extracts as green corrosion inhibitors of mild steel in hydrochloric acid medium, Mater. Res. Express 6 (2019) 106579.
[21] O. D'Alessandro, G.J. Selmi, C. Deyá, A. Di Sarli, R. R., formulation and assessment of a wash-primer containing lanthanum "Tannate" for steel temporary protection, J. of Materi Eng and Perform 27 (2018) 687–704.
[22] S. Martinez, Inhibitory mechanism of mimosa tannin using molecular modeling and substitutional adsorption isotherms, Mater. Chem. Phys. 77 (2002) 97–102.
[23] R.S. Peres, E. Cassel, C.A. Ferreira, D.S. Azambuja, Black wattle tannin as a zinc phosphating coating sealer, Surf. Interface Anal. 46 (2014) 1–6.
[24] A.A. Rahim, E. Rocca, J. Steinmetz, M.J. Kassim, R. Adnan, M.M. Sani Ibrahim, Mangrove tannins and their flavanoid monomers as alternative steel corrosion inhibitors in acidic medium, Corros. Sci. 49 (2007) 402–417.
[25] H. Gerengi, H.I. Sahin, Schinopsis lorentzii extract As a green corrosion inhibitor for low carbon steel in 1 m HCl solution, Ind. Eng. Chem. Res. 51 (2012) 780–787.
[26] O. D'Alessandro, G.J. Selmi, C. Deyá, A.R. Di Sarli, R. Romagnoli, Lanthanum derivative from "tara" tannin for steel temporary protection, Ind. Eng. Chem. Res. 57 (2018) 3215–3226.
[27] S. Flores Merino, J.J. Caprari, L. Vasquez Torres, L. Figueroa Ramos, A.A. Hadzich Girola, Inhibitive action of tara tannin in rust converter formulation, Anti-corrosion Methods Mater. 64 (2017) 136–147.
[28] A. Hadzich, S. Flores, C.J. J, R. Romagnoli, Study of zinc tannates prepared with Tara powder (Caesalpinia spinosa) as anticorrosive pigments in alkyd paints and wash primer formulations, Prog. Org. Coat. 117 (2018) 35–46.
[29] G. Matamala, W. Smeltzer, G. Droguett, Comparison of steel anticorrosive protection formulated with natural tannins extracted from acacia and from pine bark, Corros. Sci. 42 (2000) 1351–1362.
[30] O.R. Pardini, J.I. Amalvy, A.R. Di Sarli, Formulation and testing of a waterborne primer containing chestnut tannin, J. Coat. Technol. 73 (2001) 99–106.
[31] M.S. Noor Idora, L.K. Quen, H.S. Kang, Effect of tannin from Rhizophora apiculate as corrosion inhibitor for epoxy paint on mild steel, Journal of Physics: Conference Series 890 (2017) 012062.
[32] H. Gerengi, A. Jazdzewska, M. Kurtay, A comprehensive evaluation of mimosa extract as a corrosion inhibitor on AA6060 alloy in acid rain solution: part I. Electrochemical AC methods, J. Adhes. Sci. Technol. 29 (2015) 36–48.
[33] L. Guedes, K. Bacca, N. Lopes, E. Costa, Tannin of Acacia mearnsii as green corrosion inhibitor for AA7075-T6 aluminum alloy in acidic medium, Mater. Corros. 70 (2019) 1288–1297.
[34] J.V. Nardeli, C.S. Fugivara, M. Taryba, E.R.P. Pinto, M.F. Montemor, A.V. Benedetti, Tannin: A natural corrosion inhibitor for aluminum alloys, Prog. Org. Coat. 135 (2019) 368–381.
[35] S. Yahya, A.A. Rahim, A. Mohd Shah, R. Adnan, Inhibitive behaviour of corrosion of aluminium alloy in NaCl by mangrove tannin, Sains Malays. 40 (2011) 953–957.
[36] N.J.N. Nnaji, N.O. Obi-Egbedi, C.O.B. Okoye, Cashew nut testa tannin: assessing its effects on the corrosion of aluminium in HCl, Port. Electrochim. Acta 32 (2014) 157–182.
[37] N.J.N. Nnaji, C.O.B. Okoye, N.O. Obi-Egbedi, M.A. Ezeokonkwo, J.U. Ani, Spectroscopic characterization of red onion skin tannin and it's use as alternative aluminium corrosion Inhibitor in hydrochloric acid solutions, Int. J. Electrochem. Sci. 8 (2013) 1735–1758.
[38] D.R. Gabe, Principles of Metal Surface Treatment and Protection, Pergamon Press, 1978.
[39] U. SAICA, Leather Tanning Agents, in, (2019).
[40] Determination of Tannin Matter Absorbable by Hide Powder, SLC-117, (1996).
[41] O. Folin, W. Denis, On phosphotungstic-phosphomolybdic compounds as color reagents, J. Biol. Chem. 12 (1912) 239–243.
[42] V.L. Singleton, J.A. Rossi, Colorimetry of total phenolics with phosphomolybdic-phosphotungstic acid reagents, Am. J. Enol. Vitic. 16 (1965) 144–158.
[43] V. Branzoi, F. Golgovici, F. Branzoi, Aluminium corrosion in hydrochloric acid solutions and the effect of some organic inhibitors, Mater. Chem. Phys. 78 (2003) 122–131.
[44] Standard Practice for Testing Water Resistance of. Coatings in 100% Relative Humidity, ASTM D. 2247, ASTM, West Conshohocken, PA, United State, 2015.
[45] Standard Practice for Measuring Adhesion by Tape Test, ASTM D 3359, ASTM, West Conshohocken, PA, United States, 2009.
[46] Standard Test Method for Evaluating Degree of Blistering of Paints, ASTM D 714 ASTM, West Conshohocken, PA, United States, 2002.
[47] J.R. Davis, Corrosion testing, in: J.R. Davis (Ed.), Corrosion of Aluminum and Aluminum Alloys, ASM International, Materials Park, OH, 1999, pp. 219–250.
[48] M.I. Karyakina, E. Kuzmak, Protection by organic coatings: criteria, testing methods and modelling, Prog. Org. Coat. 18 (1990) 325–388.
[49] G.W. Walter, A critical review of d.c. Electrochemical tests for painted metals, Corros. Sci. 26 (1986) 39–47.
[50] W.A. Arismendi, A.E. Ortiz-Ardila, C.V. Delgado, L. Lugo, L.G. Sequeda-Castañeda, C.A. Celis-Zambrano, Modified tannins and their application in wastewater treatment, Water Sci. Technol. 78 (2018) 1115–1128.
[51] F. dos Santos Grasel, M. Flôres Ferrão, C.R. Wolf, Development of methodology for identification the nature of the polyphenolic extracts by FTIR associated with multivariate analysis, Spectrochim. Acta A. Mol. Biomol. Spectrosc. 153 (2016)

94–101.
[52] A. Ricci, K.J. Olejar, G.P. Parpinello, P.A. Kilmartin, A. Versari, Application of Fourier Transform Infrared (FTIR) Spectroscopy in the characterization of tannins, Appl. Spectrosc. Rev. 50 (2015) 407–442.
[53] P.S. Santos, H.S. Santos, S.P. Toledo, Standard transition aluminas, Electron microscopy studies, Materials Research 3 (2000) 104–114.
[54] M. Yurtsever, I.A. Sengil, Biosorption of Pb(II) ions by modified quebracho tannin resin, J. Hazard. Mater. 163 (2009) 58–64.
[55] M. Taghavikish, N.K. Dutta, N. Roy Choudhury, Emerging corrosion inhibitors for interfacial coating, Coatings 7 (2017) 217–245.
[56] F. Trombetta, F.R. Souza, M.O. Souza, B.C. Borges, A.F. Panno, E.M.A. Martini, Stability of aluminum in 1-butyl-3-methylimidazolium tetra fluoroborate ionic liquid and ethylene glycol mixtures, Corros. Sci. 53 (2011) 51–58.
[57] B.A. Abd-El-Naby, O.A. Abdullatef, W.A. El-Mahmody, Effect of surfactants on the corrosion behavior of aluminum in acid solutions containing chloride ions, Phys. Chem. 7 (2017) 1–7.
[58] K. Mansouri, K. Ibrik, N. Bensalah, A. Abdel-Wahab, Anodic dissolution of pure aluminum during electrocoagulation process: influence of supporting electrolyte, initial pH, and current density, Ind. Eng. Chem. Res. 50 (2011) 13362–13372.
[59] F.Sd. Silva, J. Bedoya, S. Dosta, N. Cinca, I.G. Cano, J.M. Guilemany, A.V. Benedetti, Corrosion characteristics of cold gas spray coatings of reinforced aluminum deposited onto carbon steel, Corros. Sci. 114 (2017) 57–71.
[60] Y. Solhan, N.K. Othman, A.R. Daud, A. Jalar, Effect of scan rate on corrosion inhibition of carbon steel in the presence of rice straw extract - potentiodynamic studies, Sains Malays. 43 (2014) 1083–1087.
[61] X.L. Zhang, Z.H. Jiang, Z.P. Yao, Y. Song, Z.D. Wu, Effects of scan rate on the potentiodynamic polarization curve obtained to determine the Tafel slopes and corrosion current density, Corros. Sci. 51 (2009) 581–587.
[62] N. Rezaee, M.M. Attar, B. Ramezanzadeh, Studying corrosion performance, microstructure and adhesion properties of a room temperature zinc phosphate conversion coating containing Mn2+ on mild steel, Surf. Coat. Technol. 236 (2013) 361–367.
[63] A. Scoton, A. Chinelatto, E.Md.J. Agnolon Pallone, A.M. de Souza, M. Kowalczuk Manosso, A.L. Chinelatto, R. Tomasi, Mechanisms of microstructure control in conventional sintering, in: A. Lakshmanan (Ed.), Sintering of Ceramics - New Emerging Techniques, Intech, 2012, p. 24 Rijeka, Croatia.